HHS Public Access

Author manuscript

Odontology. Author manuscript; available in PMC 2018 July 01.

Published in final edited form as:

Odontology. 2017 July ; 105(3): 354–363. doi:10.1007/s10266-016-0268-z.

Novel bioactive tetracycline-containing electrospun polymer fibers as a potential antibacterial dental implant coating

R. G. Shahi[1,4], **M. T. P. Albuquerque**[1], **E. A. Münchow**[1], **S. B. Blanchard**[4], **R. L. Gregory**[1], and **M. C. Bottino**[1,2,3,*]

[1]Department of Biomedical & Applied Sciences, Division of Dental Biomaterials, Indiana University School of Dentistry (IUSD), Indianapolis, IN, 46202, USA

[2]Department of Biomedical Engineering, Indiana University Purdue University, Indianapolis, IN, 46202, USA

[3]Department of Anatomy & Cell Biology, Indiana University School of Medicine, Indianapolis, IN, 46202, USA

[4]Department of Periodontics & Allied Dental Programs, IUSD, Indianapolis, IN, 46202, USA

Abstract

The purpose of this investigation was to determine the ability of tetracycline-containing fibers to inhibit biofilm formation of peri-implantitis-associated pathogens [*i.e.*, *Porphyromonas gingivalis* (*Pg*), *Fusobacterium nucleatum* (*Fn*), *Prevotella intermedia* (*Pi*), and *Aggregatibacter actinomycetemcomitans* (*Aa*)]. Tetracycline hydrochloride (TCH) was added to a poly(DL-lactide) [PLA], poly(ε-caprolactone) [PCL], and gelatin [GEL] polymer blend solution at distinct concentrations to obtain the following fibers: PLA:PCL/GEL (TCH-free, control), PLA:PCL/GEL +5%TCH, PLA:PCL/GEL+10%TCH, and PLA:PCL/GEL+25%TCH. The inhibitory effect of TCH-containing fibers on biofilm formation was assessed by colony-forming units (CFU/mL). Qualitative analysis of biofilm inhibition was done via scanning electron microscopy (SEM). Statistical significance was reported at $p<0.05$. Complete inhibition of biofilm formation on the fibers was observed in groups containing TCH at 10 and 25 wt.%. Fibers containing TCH at 5 wt. % demonstrated complete inhibition of *Aa* biofilm. Even though a marked reduction in CFU/mL was observed with an increase in TCH concentration, *Pi* proved to be the most resilient microorganism. SEM images revealed the absence of or a notable decrease in bacterial biofilm on the TCH-containing nanofibers. Collectively, our data suggests that tetracycline-containing fibers hold great potential as an antibacterial dental implant coating.

Keywords

tetracycline; nanofibers; implant; coating; peri-implantitis

Correspondence to: Marco C. Bottino, DDS, PhD, Assistant Professor, Indiana University School of Dentistry, Department of Biomedical & Applied Sciences, 1121 W. Michigan St. (DS270B), Indianapolis, IN, 46202, USA, Tel: +1-317-274-3725; fax: +1-317-278-7462, mbottino@iu.edu.

Conflict of interest The authors declare that they have no conflict of interest.

Introduction

Osseointegrated titanium (Ti) implants have been used for decades and are considered a safe and predictable clinical therapy to replace missing teeth in partial and completely edentulous patients [1, 2]. Despite significant advances in implant surface science [3–5], particularly related to the positive role played by implant surface texture on bone integration [5, 6], the risk of infection and early implant failure still is a major clinical concern [7–11]. A recent meta-analysis indicates that there is some evidence of an increased number of implant failures and bone loss around implants (*e.g.*, peri-implantitis) associated with periodontally-compromised patients as compared to healthy individuals [11].

Peri-implantitis is defined as a progressive and irreversible polymicrobial infection and clinically characterized by soft tissue inflammation, bleeding and/or suppuration and rapid bone loss around dental implants [7, 8]. Subgingival anaerobic Gram-negative bacteria (e.g., *Pi*, *Aa*, and *Pg*), normally associated with periodontitis, are also related with peri-implantitis [7, 8]. Suffice it to say, once peri-implantitis is established, one needs to focus on decontamination of the implant surfaces, control of inflammation, inhibition of progressive bone loss, and potential regeneration of lost peri-implant bone. Over the years, besides the traditional non-surgical and surgical methods of treatment, novel and innovative therapeutics, for example those involving laser and photodynamic therapies have been tested with varying degrees of success [12, 13].

Remarkable progress in the field of nanotechnology has propelled materials research toward the development of bioactive antibacterial strategies [14, 18] that could be potentially used as a prophylactic approach to avoid early implant infection. Among a wide variety of therapeutic agents, tetracycline has been clinically used to disinfect contaminated implant surfaces [19, 20]. Tetracycline (TCH) is a protein synthesis inhibitor that binds to the bacterial 30S ribosome subunit and blocks the bond between tRNA and mRNA [21]. Notably, TCH has demonstrated its ability to not only function as an effective broad-spectrum antibiotic against periodontitis and peri-implantitis-associated microbes (*e.g.*, *Pg, Fn, Pi,* and *Aa*), but more importantly, it has been proven to increase fibroblastic cell proliferation [19] and inhibit collagenase activity [22]. Nonetheless, even though overwhelming amounts of research have been done to enhance/accelerate implant integration [3–6], very little work has been conducted to develop an antibacterial dental implant coating [23, 24].

In recent years, electrospinning, a nanotechnology-based technique, has been demonstrated to be an extremely feasible route to synthesize bioactive polymer nanofibers capable of sustained release of therapeutic antimicrobial drugs (*e.g.*, metronidazole, ciprofloxacin, and minocycline, among others) [14–18]. Interestingly, hydroxyapatite-incorporated polymer nanofibers have been used to modify the surface of titanium implants, aiming to improve osseointegration [25]. Nonetheless, no single dental implant with antimicrobial surface properties is currently available. Therefore, there is a significant potential to develop an antibiotic-containing nanofiber-based polymer coating to minimize early implant loss, especially in periodontally-compromised patients. Thus, the present study aimed to synthesize tetracycline-containing fibers capable of inhibiting the growth of peri-implantitis-

associated pathogens as the first step towards development of an antimicrobial dental implant coating.

Materials and methods

Materials

Four distinct peri-implantitis-associated Gram-negative anaerobic bacteria were selected for this study. *Pg* (ATCC 33277), *Fn* (ATCC 10953), *Pi* (ATCC 25611), and *Aa* (ATCC 33384) were procured from the American Type Culture Collection (ATCC, Manassas, VA, USA).

Poly(DL-lactide) (PLA, inherent viscosity: 0.55–0.75 dL/g in $CHCl_3$) and poly(ε-caprolactone) (PCL, inherent viscosity: 1.29 dL/g in $CHCl_3$) were purchased from Lactel Absorbable Polymers (Durect Corporation, Birmingham, AL, USA). Type-B Gelatin (GEL) from bovine skin (bloom no. 225), tetracycline hydrochloride (TCH, molecular weight [Mw] 480.90 g/mol), hexamethyldisilazane (HMDS), formaldehyde, and 1,1,1,3,3,3-hexafluoro-2-propanol (HFP) were acquired from Sigma-Aldrich (Sigma-Aldrich Corporation, St. Louis, MO, USA). Brain heart infusion (BHI, Difco Laboratories Inc., Detroit, MI, USA) culture media containing 5 g/L yeast extract (BHI-YE, Difco Laboratories Inc., Detroit, MI, USA) with 5% v/v Vitamin K/hemin (Thermo Fisher Scientific, Inc., Pittsburgh, PA, USA) solution was used. Phosphate-buffered saline, ethanol, and blood agar plates supplemented with 5% sheep blood were obtained from Fisher Scientific Company LLC (Fair Lawn, NJ, USA).

Synthesis and Morphological Characterization of Tetracycline-containing Fibers

In this *in vitro* study, TCH-containing polymer fibers were synthesized via electrospinning using a laboratory-based system [14–18]. A syringe pump (Legato 200 KD Scientific Inc., Holliston, MA, USA), a high-voltage source (ES50P-10W/DAM, Gamma High-Voltage Research, Inc., Ormond Beach, FL, USA), and a grounded stainless steel collecting drum (ϕ = 4 cm) connected to a high-speed mechanical stirrer (BDC6015 Caframo, Wiarton, ON, CA) were used to process defect-free (*i.e.*, bead-free) fibers. PLA, PCL, and GEL were dissolved in HFP (mass ratio of 2:2:1) overnight and under vigorous stirring to obtain a 75 mg/mL blended polymer solution. Subsequently, TCH was individually incorporated at distinct concentrations (5, 10, and 25 wt.%, respective to the total polymer blend weight, *i.e.*, 450 mg in 6 mL of HFP) and stirred for 24 h before being electrospun into fibers. One control (TCH-free) and three experimental (TCH-containing) fiber groups were spun. The pure polymer blend (PLA:PCL/GEL) or the TCH-containing polymer solutions were individually loaded into plastic syringes (Becton-Dickinson, Franklin Lakes, NJ, USA) fitted with a metallic blunt end 27G needle. The polymer mixtures (4 mL) were then processed under optimized conditions (*i.e.*, 1 mL/hr, 18-cm distance, and 18–22 kV) on an aluminum foil-covered rotating (120 rpm) mandrel at room temperature (RT). The electrospun fibers were placed in a desiccator for 24 h to ensure complete elimination of any remaining solvents. The electrospun fibers were morphologically characterized via scanning electron microscopy (SEM, JSM-5310LV, JEOL, Tokyo, Japan). The average fiber diameter was calculated from three distinct SEM images by measuring the diameter of 40 fibers per image (n=120 fibers/group) using a dedicated software (ImageJ 1.44i, National Institutes of Health,

Bethesda, MD, USA) [14–18]. High-performance liquid chromatography (HPLC) was used to evaluate TCH release profile from antibiotic-incorporated nanofibers [14]. In brief, TCH-containing electrospun samples (15 × 15 mm^2, n=4/group) were weighed and incubated in 10 mL of PBS at 37°C. 1 mL aliquots were retrieved at different time intervals and replenished with equivalent amounts of fresh PBS. The TCH content (absorption peak 276.8 nm) was determined using HPLC equipped with a UV-Vis detector (Perkin-Elmer, Shelton, CT, USA). TCH solutions at known concentrations were used to obtain the calibration curves [14].

Biofilm Inhibition Assay

The inhibitory effects of TCH-containing fibers on the biofilm growth of four periimplantitis-associated pathogens, *i.e., Pg, Fn, Pi, and Aa*, were evaluated using a previously well-characterized biofilm inhibition assay [16–18]. Electrospun samples (n=10/group/bacteria) were cut (15 × 15 mm^2) from the synthesized fibrous mats, mounted in a plastic cell culture device (CellCrown™, Scaffdex, Tampere, Finland), and placed in 24-well plates [18]. The samples tested included the three TCH-containing experimental groups (*i.e.*, PLA:PCL/GEL+5wt.%TCH, PLA:PCL/GEL+10wt.%TCH, PLA:PCL/GEL+25wt.%TCH), and the control (*i.e.*, pure PLA:PCL/GEL). Electrospun samples were disinfected with 2 mL of 70% ethanol for 30 min and rinsed (2×) with 2 mL of sterile 0.9% saline. All bacteria were cultured at 37°C for 48 h in 5 mL of BHI-YE in an anaerobic GasPak jar [18]. 50-μL of the 48 h bacterial suspensions (*ca.* 10^6 bacteria) was inoculated into each well with 2 mL of the growth media. Following the incubation period, the electrospun samples were removed from the wells using sterile forceps, washed gently (2×) with 1 mL of 0.9% saline and suspended in 2 mL of 0.9% saline, followed by sonication (10 s) and vortexing (30 s) [18]. The dislodged biofilm bacteria were plated onto anaerobic blood agar plates using a conventional spiral plater system [18]. For each sample, two dilutions were plated, one undiluted and one diluted (1:100). The plates were incubated under anaerobic conditions for 48 h prior to evaluation using an automated colony counter (Synbiosis Design/Build, LLC, Frederick, MD, USA) to determine the colony-forming units (CFU/mL) to be compared with the data obtained from the TCH-free fibers [18]. Bacterial growth inhibition of the TCH-containing fibers and the control was qualitatively assessed using a scanning electron microscope (SEM). In brief, two additional samples per group were tested under the same protocol. After incubation, the samples were harvested, washed with PBS to remove unbound bacteria, and fixed in buffered 4% formaldehyde. After dehydration, using ascending ethanol gradients, and soaking in ethanol/hexamethyldisilazane gradients, samples were mounted on Al stubs, sputter-coated with gold and imaged using SEM [18].

Statistical analyses

Results are shown as the mean value plus or minus the standard deviation (±SD) of the mean. One-way ANOVA, followed by Tukey's multiple comparisons, were used to evaluate the groups for differences in fiber diameter. A comparison between the groups for differences in bacterial counts was made using the Wilcoxon Rank Sum tests. A 5% significance level was used.

Results

A representative SEM image of the 25 wt.% TCH-containing nanofibers is shown in Fig. 1A; all groups demonstrated similar fiber morphology, regardless of the presence and concentration of TCH. Overall, regardless of the presence of TCH, a three-dimensional nanofibrous network with micron-sized pores was seen. The mean fiber diameter for all fibers ranged from 172 to 393 nm (Fig. 1B). The greatest mean fiber diameter was found in the 25 wt.%TCH-containing group (324±69 nm), followed in descending order by 10 wt.%TCH (249±72 nm), 5 wt.%TCH (244±66 nm), and the control (221±49 nm). Regarding the mean drug release ability of the TCH-containing fibers, the greater the TCH content, the more TCH was released (Fig. 2A). All experimental groups displayed a burst release of TCH.

Pure PLA:PCL/GEL (TCH-free, control group) allowed significant biofilm formation as demonstrated by high colony-forming units ($\log_{10}$ CFU/mL) values (Fig. 2B) for all bacteria (*Pi* = 5.4; *Pg* = 5.6; *Aa* = 5.1; *Fn* = 3.7). Meanwhile, all TCH-containing fibers displayed antibacterial effects when compared to the control (Fig. 2B). All TCH-containing fibers significantly inhibited the growth of *Aa*. The control fibers had significantly ($p=0.0001$) higher bacteria counts than 5, 10, and 25 wt.%TCH. However, 5 wt.% was not significantly different from 10 or 25 wt.% ($p>0.05$). For *Fn*, the control group had a significantly higher count than the experimental groups. Worth mentioning, significant differences ($p\leq0.0002$) in biofilm reduction were seen as a function of the TCH content, where increasing the TCH amount led to higher biofilm reduction. In the case of *Pg*, the control group had a significantly higher count than 5, 10, and 25 wt.%. Similar to *Fn*, 5 wt.%TCH had significantly ($p\leq0.0208$) higher counts than 10 and 25 wt.%; however, 10 and 25 wt.% were not statistically different ($p>0.05$). Lastly, for *Pi*, the control group had a significantly ($p=0.0002$) higher count than 5, 10, and 25 wt.%. TCH incorporation at 25 wt.% had significantly lower counts than 5 wt.%TCH ($p=0.0002$) and 10 wt.%TCH ($p=0.0017$). No statistically significant difference ($p=0.91$) was seen between 5 and 10 wt.%TCH for *Pi*. Taken together, *Pi* biofilm demonstrated being the most resilient; however, there was a marked reduction in CFU/mL, with an increase in TCH concentration.

SEM imaging was carried out as a qualitative method to confirm the presence/absence of bacterial biofilm. SEM images obtained after biofilm exposure clearly demonstrated large and dense clusters for all examined bacteria (*Pg, Fn, Pi,* and *Aa*) throughout the TCH-free (control) electrospun fibers (Figs. 3A, 4A, 5A, and 6A). All the experimental groups exhibited an absence or a notable decrease in bacteria biofilm. Electrospun fibers containing TCH at 10 and 25 wt.% revealed complete elimination of *Pg* and *Fn* biofilms on the fibers (Figs. 3 and 4); however, few bacteria were observed on the surface of the 5 wt.% fibers (Figs. 3B and 4B). It is interesting to note that the characteristic morphology (*i.e.*, spindle-shaped) of *Fn* bacteria was clearly identified within the control group. Fig. 4A shows a representative SEM image, in which 30 measurements were taken of the diameter of the spindle-shaped bacteria. The mean *Fn* diameter was 487±159 nm, more than two-fold greater than the diameter of the TCH-free polymer fibers (221±49 nm). No evidence of *Aa* bacteria biofilm was found on the surfaces of any TCH-containing fibers. A notable decrease of *Pi* bacteria biofilm was seen as the concentration of TCH increased (Fig. 6).

Discussion

In the past few years, the application of electrospun fibers as a delivery system of distinct drugs to aid an antibacterial property to metallic orthopedic implants has gained increased attention [23, 24]. Nevertheless, and to the best of our knowledge, TCH has so far never been considered in the fabrication of an alternative antimicrobial nanofibrous-based biodegradable dental implant coating. Taking into consideration that TCH is a broad-spectrum antibiotic with well-known activity against periodontitis- and peri-implantitis-associated microbes, the present study carries a strong clinical relevance in implant dentistry.

This *in vitro* study investigated the ability of TCH-containing polymer nanofibers to inhibit the growth of peri-implantitis-associated bacteria. Overall, the TCH-containing fibers exhibited a homogeneous architecture and satisfactory morphology (Fig. 1A). Hence, there were no clear differences between the TCH-containing and control (TCH-free) fibers, except for a slight increase in fiber diameter noted for the highest concentrated group (25 wt. %TCH, Fig. 1B). At the moment, it can be speculated that the presence of hydroxyl groups in the molecular structure of TCH increased the viscosity of the polymer solution due to the increase in intermolecular (*e.g.*, hydrogen bonding) interactions [26], which has probably affected the chain entanglement process during electrospinning, resulting in thicker fibers. Despite the absence of morphological differences between the synthesized fibers, all TCH-containing fibers were able to inhibit or dramatically reduce biofilm growth (Fig. 2B) when compared to the control, which displayed the highest counts of viable cells on biofilms, thus supporting the potential use of these bioactive fibers as surface coating for titanium dental and orthopedic implants.

It is well-established in the literature that the presence of biofilm surrounding implant sites is a common reason, but not the only one, for early implant loss or peri-implantitis, especially in periodontally-compromised high-risk individuals [11]. Knowing that dental implants lack antibacterial properties and considering that they have an intrinsically rough and irregular surface topography, biofilm elimination is a very difficult task. According to the findings of the present study, modification of the titanium implants' surface with TCH-containing polymer nanofibers holds great promise toward combating/controlling the accumulation of biofilm. Herein, both the TCH concentration and bacterial species tested significantly influenced the anti-biofilm effect. Overall, the most concentrated fibers (25 wt.%TCH) resulted in higher biofilm inhibition on the fibers, as compared to the less concentrated fibers (5 wt.%TCH), probably due to the release of greater amounts of the drug in the former group than in the latter (Fig. 2A) [16, 17]; the only exception was observed against *Aa*, in which all the TCH-containing fibers were able to completely inhibit biofilm growth, regardless of the TCH concentration (Fig. 2B). The higher susceptibility of *Aa*, even at low TCH concentration, can be explained by the low minimal inhibitory concentration (MIC) of tetracycline-based compounds against this bacterium, as suggested by a previous study [27]. Conversely, *Pi* demonstrated the lowest susceptibility to TCH, since even the 25 wt.%TCH group did not promote complete biofilm elimination. In this case, it is important to note that *Pi* has been reported to encode different copies of beta-lactamases and multidrug/efflux transporters, which provide resistance to antibiotics [28]. Furthermore, it can be speculated that the MIC of TCH would be greater against *Pi* compared to the other species. This has

been demonstrated by van Winkelhoff et al. [29] who reported that the MIC of tetracycline against *Pi, Fn, Aa*, and *Pg* was 2.0, 0.5, 0.19 and 0.023 mg/L, respectively. Consequently, *Pi* seems to be a more challenging pathogen to eliminate.

Another interesting finding of the present study is that increasing the concentration of TCH from 10 to 25 wt.% did not result in any positive (dose-dependent) effect in biofilm inhibition against the more susceptible bacteria species tested (*i.e.*, *Pg, Aa*, and *Fn*) (Fig. 2B). This is important to know, because the greater the content of TCH used, the greater the probability of increasing cytotoxic effects and bacterial resistance. According to the present results, the amount of TCH used for the preparation of the 10 wt.%TCH fibers was approximately 45 mg. However, it is worth mentioning that the real amount of TCH added into each fiber is much lower than this, since 45 mg was the total amount of the drug added into 6 mL of the polymer solution, which resulted in hundreds of thousands of fibers (Fig. 1). In light of this, it can be inferred that even very low amounts of TCH are able to reduce susceptible bacteria, such as *Pg*, *Aa*, and *Fn*. Once again, the same pattern could not be extrapolated to the less susceptible bacteria tested (*i.e.*, *Pi*), which, even after contact with the most concentrated (25 wt.%) fibers, biofilm was not completely eliminated. In fact, this may corroborate with recent literature that indicated *Pi* is one of the most common pathogens found in peri-implantitis [30, 31].

Taken together, successful TCH release from the electrospun polymer fibers was confirmed both by the HPLC data and, more importantly, by the significant reduction in bacterial biofilm. It is well-known that TCH acts inhibiting bacterial protein synthesis by preventing the association of aminoacyl-tRNA with the bacterial ribosome. Moreover, a recent study highlighted the antimicrobial action of TCH due to its ability to bind to various bacterial RNAs in alternative binding modes or sites, consequently disorganizing the biofilm structure [32].

SEM analysis of the fibers after the biofilm assay corroborates with the CFU/mL data, which indicates the presence of bacterial structures with different shapes/sizes (depending on the bacterial species) compared to the fibers could be easily observed on the TCH-free fibers (control). On the other hand, the presence of some bacteria could not be easily detected on the surface of the TCH-incorporated fibers, thus confirming the inhibitory effects. Only for the *Pi* group was the presence of some bacterial cells detected, even around the TCH-containing fibers, since the biofilm was not completely eliminated within this group (Fig. 6).

Conclusion

Our ongoing research focuses on synthesizing antibiotic-containing nanofibers on titanium dental implants [33] to first study *in vitro* the antimicrobial properties against a multispecies peri-implantitis-relevant biofilm, and later to evaluate its effects on a pre-clinical animal model. Taken together, this study demonstrated that antibiotic-containing fibers can effectively inhibit peri-implantitis-related biofilm formation, suggesting that tetracycline fibers hold great potential as an antibacterial implant coating.

Acknowledgments

This study was performed as part of the requirements for the MSD in Periodontics at IU School of Dentistry (IUSD). This work was partially supported by a grant from Delta Dental Foundation to Dr. Rana G. Shahi. M.C.B. acknowledges funding support from IUSD and the NIH-NIDCR (Grant # DE023552). The authors thank Mr. George Eckert, Indiana University School of Medicine, for his statistical analyses.

References

1. Brånemark PI, Adell R, Breine U, Hansson BO, Lindström J, Ohlsson A. Intraosseous anchorage of dental prostheses. I. Experimental studies. Scand J Plast Reconstr Surg. 1969; 3:81–100. [PubMed: 4924041]
2. Adell R, Lekholm U, Rockler B, Branemark PI. A 15-year study of osseointegrated implants in the treatment of the edentulous jaw. Int J Oral Surg. 1981; 10:387–416. [PubMed: 6809663]
3. Le Guéhennec L, Soueidan A, Layrolle P, Amouriq Y. Surface treatments of titanium dental implants for rapid osseointegration. Dent Mater. 2007; 23:844–54. [PubMed: 16904738]
4. Mendonça G, Mendonça DB, Aragão FJ, Cooper LF. Advancing dental implant surface technology--from micron- to nanotopography. Biomaterials. 2008; 29:3822–35. [PubMed: 18617258]
5. Coelho PG, Jimbo R, Tovar N, Bonfante EA. Osseointegration: hierarchical designing encompassing the macrometer, micrometer, and nanometer length scales. Dent Mater. 2015; 31:37–52. [PubMed: 25467952]
6. Mendonça G, Mendonça DB, Simões LG, Araújo AL, Leite ER, Duarte WR, Aragão FJ, Cooper LF. The effects of implant surface nanoscale features on osteoblast-specific gene expression. Biomaterials. 2009; 30:4053–62. [PubMed: 19464052]
7. Mombelli A, Décaillet F. The characteristics of biofilms in peri-implant disease. J Clin Periodontol. 2011; 38(Suppl 11):203–13. [PubMed: 21323716]
8. Mombelli A, Muller N, Cionca N. The epidemiology of peri-implantitis. Clin Oral Implants Res. 2012; 23(suppl 6):67–76.
9. Monje A1, Alcoforado G, Padial-Molina M, Suarez F, Lin GH, Wang HL. Generalized aggressive periodontitis as a risk factor for dental implant failure: a systematic review and meta-analysis. J Periodontol. 2014; 85:1398–407. [PubMed: 24835415]
10. Heitz-Mayfield LJ, Mombelli A. The therapy of peri-implantitis: a systematic review. Int J Oral Maxillofac Implants. 2014; 29(Suppl):325–45. [PubMed: 24660207]
11. Chrcanovic BR, Albrektsson T, Wennerberg A. Periodontally compromised vs. periodontally healthy patients and dental implants: a systematic review and meta-analysis. J Dent. 2014; 42:1509–27. [PubMed: 25283479]
12. Mailoa J, Lin GH, Chan HL, MacEachern M, Wang HL. Clinical outcomes of using lasers for peri-implantitis surface detoxification: a systematic review and meta-analysis. J Periodontol. 2014; 85:1194–202. [PubMed: 24476547]
13. Bassetti M, Schär D, Wicki B, Eick S, Ramseier CA, Arweiler NB, Sculean A, Salvi GE. Anti-infective therapy of peri-implantitis with adjunctive local drug delivery or photodynamic therapy: 12-month outcomes of a randomized controlled clinical trial. Clin Oral Implants Res. 2014; 25:279–87. [PubMed: 23560645]
14. Albuquerque MT, Ryan SJ, Münchow EA, Kamocka MM, Gregory RL, Valera MC, Bottino MC. Antimicrobial effects of novel triple antibiotic paste-mimic scaffolds on Actinomyces naeslundii biofilm. J Endod. 2015 Apr 24. pii: S0099-2399(15)00237-X Epub ahead of print. doi: 10.1016/j.joen.2015.03.005
15. Albuquerque MT, Valera MC, Moreira CS, Bresciani E, de Melo RM, Bottino MC. Effects of ciprofloxacin-containing scaffolds on Enterococcus faecalis biofilms. J Endod. 2015; 41:710–4. [PubMed: 25698261]
16. Waeiss RA, Negrini TC, Arthur RA, Bottino MC. Antimicrobial effects of drug-containing electrospun matrices on osteomyelitis-associated pathogens. J Oral Maxillofac Surg. 2014; 72:1310–9. [PubMed: 24630157]

17. Bottino MC, Arthur RA, Waeiss RA, Kamocki K, Gregson KS, Gregory RL. Biodegradable nanofibrous drug delivery systems: effects of metronidazole and ciprofloxacin on periodontopathogens and commensal oral bacteria. Clin Oral Investig. 2014; 18:2151–8.
18. Bottino MC, Kamocki K, Yassen GH, Platt JA, Vail MM, Ehrlich Y, Spolnik KJ, Gregory RL. Bioactive nanofibrous scaffolds for regenerative endodontics. J Dent Res. 2013; 92:963–9. [PubMed: 24056225]
19. Wittrig EE, Zablotsky MH, Layman DL, Meffert RM. Fibroblastic growth and attachment on hydroxyapatite-coated titanium surfaces following the use of various detoxification modalities. Part I: Noncontaminated hydroxyapatite. Implant Dent. 1992; 1:189–94. [PubMed: 1288813]
20. Wheelis SE, Gindri IM, Valderrama P, Wilson TG Jr, Huang J, Rodrigues DC. Effects of decontamination solutions on the surface of titanium: investigation of surface morphology, composition, and roughness. Clin Oral Implants Res. 2015 Jan 12. Epub ahead of print. doi: 10.1111/clr.12545
21. Connell SR, Tracz DM, Nierhaus KH, Taylor DE. Ribosomal protection proteins and their mechanism of tetracycline resistance. Antimicrob Agents Chemother. 2003; 47:3675–81. [PubMed: 14638464]
22. Wilcox JR, Covington DS, Paez N. Doxycycline as a modulator of inflammation in chronic wounds. Wounds. 2012; 24:339–49. [PubMed: 25876218]
23. Li LL, Wang LM, Xu Y, Lv LX. Preparation of gentamicin-loaded electrospun coating on titanium implants and a study of their properties in vitro. Arch Orthop Trauma Surg. 2012; 132:897–903. [PubMed: 22373914]
24. Gilchrist SE, Lange D, Letchford K, Bach H, Fazli L, Burt HM. Fusidic acid and rifampicin co-loaded PLGA nanofibers for the prevention of orthopedic implant associated infections. J Control Release. 2013; 170:64–73. [PubMed: 23639451]
25. Ravichandran R, Ng CCh, Liao S, Pliszka D, Raghunath M, Ramakrishna S, Chan CK. Biomimetic surface modification of titanium surfaces for early cell capture by advanced electrospinning. Biomed Mater. 2012; 7:015001. [PubMed: 22156014]
26. Kim YJ, Park MR, Kim MS, Kwon OH. Polyphenol-loaded polycaprolactone nanofibers for effective growth inhibition of human cancer cells. Mater Chem Phys. 2012; 133:674–680.
27. Oettinger-Barak O, Dashper SG, Catmull DV, Adams GG, Sela MN, Machtei EE, Reynolds EC. Antibiotic susceptibility of Aggregatibacter actinomycetemcomitans JP2 in a biofilm. J Oral Microbiol. 2013; 5:20320.
28. Ruan Y, Shen L, Zou Y, Qi Z, Yin J, Jiang J, Guo L, He L, Chen Z, Tang Z, Qin S. Comparative genome analysis of Prevotella intermedia strain isolated from infected root canal reveals features related to pathogenicity and adaptation. BMC Genomics. 2015; 16:122. [PubMed: 25765460]
29. van Winkelhoff AJ, Herrera D, Oteo A, Sanz M. Antimicrobial profiles of periodontal pathogens isolated from periodontitis patients in The Netherlands and Spain. J Clin Periodontol. 2005; 32:893–898. [PubMed: 15998275]
30. Albertini M, López-Cerero L, O'Sullivan MG, Chereguini CF, Ballesta S, Ríos V, Herrero-Climent M, Bullón P. Assessment of periodontal and opportunistic flora in patients with peri-implantitis. Clinical Oral Implants Research. 2014; 26:937–41. [PubMed: 24720498]
31. Casado PL, Otazu IB, Balduino A, de Mello W, Barboza EP, Duarte ME. Identification of periodontal pathogens in healthy periimplant sites. Implant Dent. 2011; 20:226–35. [PubMed: 21613949]
32. Chukwudi CU. Ribosomal RNA binding sites and the molecular mechanism of action of the tetracyclines. Antimicrob Agents Chemother. 2016 May 31. pii: AAC.00594–16 Epub ahead of print.
33. Bottino MC, Münchow EA, Albuquerque MTP, Kamocki K, Shahi R, Gregory RL, Chu TG, Pankajakshan D. Tetracycline-incorporated polymer nanofibers as a potential dental implant surface modifier. J Biomed Mater Res B Appl Biomater. 2016; Epub ahead of print. doi: 10.1002/jbm.b.33743

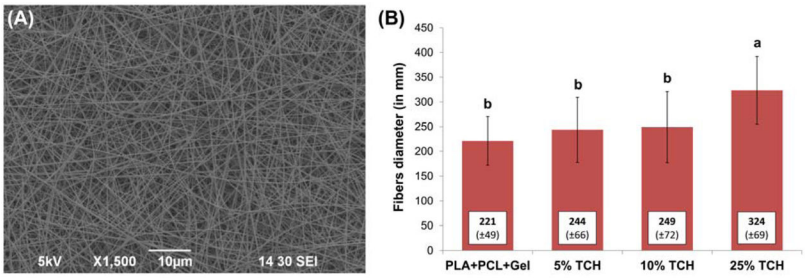

Fig. 1.

(A) Representative SEM image of the PLA:PCL/GEL+25wt.%TCH fibers. Note the three-dimensional nanofibrous network with micron-sized pores. **(B)** Mean fiber diameter (±standard deviation) for all electrospun fibers. Similar lowercase letters above bars indicate no significant differences at the P 0.05 level.

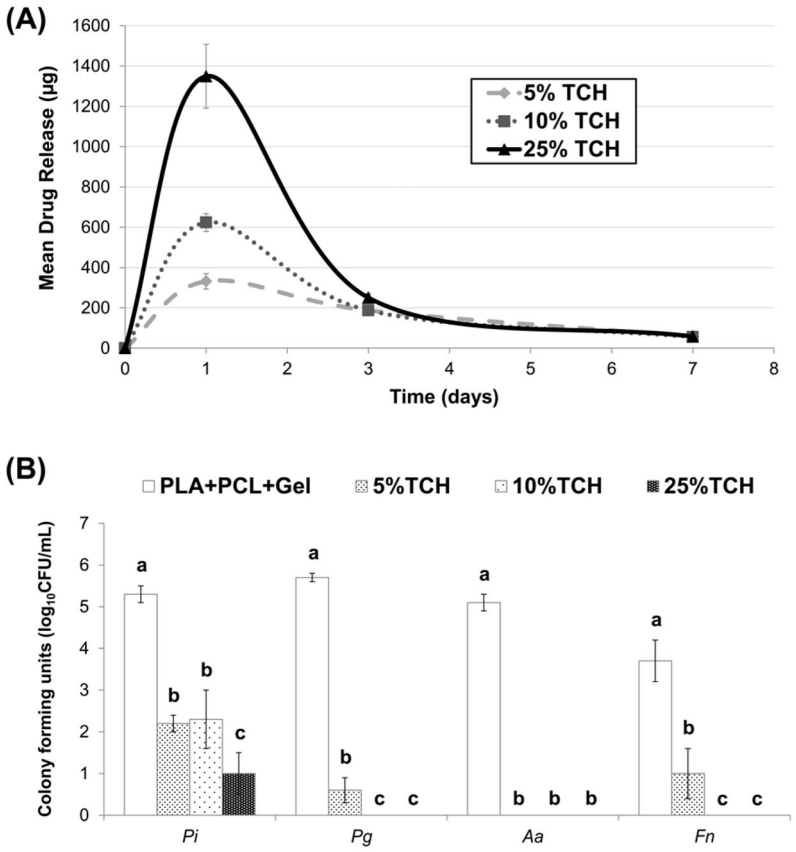

Fig. 2.

(A) Mean drug release profile of the TCH-containing groups. **(B)** Mean counts (expressed as $\log_{10}$ CFU/mL) of viable biofilm cells cultured on electrospun fibers. Distinct lowercase letters above standard deviation (SD) bars indicate statistically significant differences among fibers for the same bacteria ($p<0.05$); uppercase letters in the inset table represent statistically significant differences between bacterial species and the same fiber group ($p<0.05$).

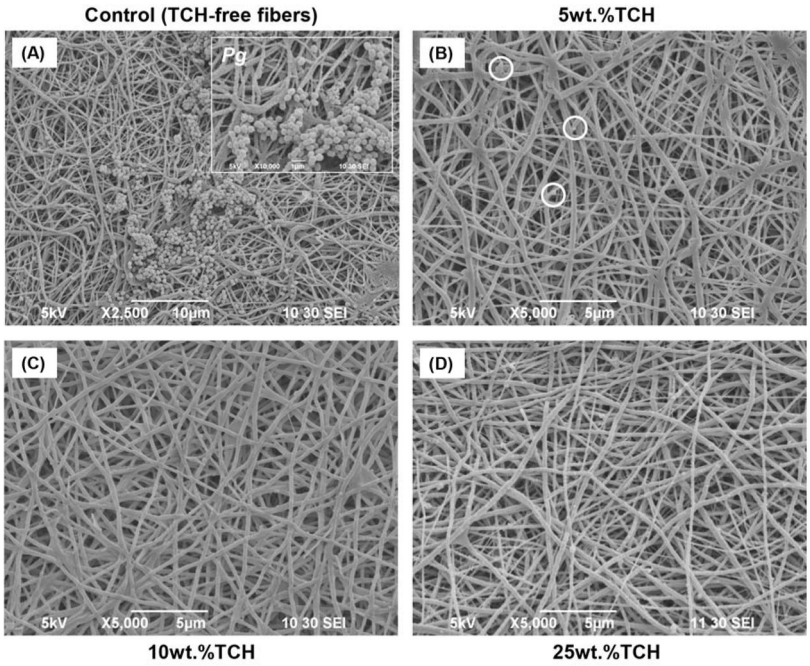

Fig. 3.

Representative SEM images of the electrospun fibers following *Pg* exposure. **(A)** control PLA:PCL/GEL [TCH-free], **(B)** PLA:PCL/GEL+5wt.%TCH, **(C)** PLA:PCL/GEL+10wt.%TCH, and **(D)** PLA:PCL/GEL+25wt.%TCH. **(A)** Note the presence of *Pg* biofilm covering most of the nanofibrous surface. Inset SEM image (10,000× magnification, scale bar = 1 μm) demonstrates the morphological aspects of *Pg*. **(B)** SEM image indicates (white circles) the presence of *Pg* bacteria only in a few areas on the 5 wt.% of TCH-containing fibers. **(C–D)** SEM images revealing complete absence of *Pg* on the fibers containing TCH at 10 and 25 wt.%.

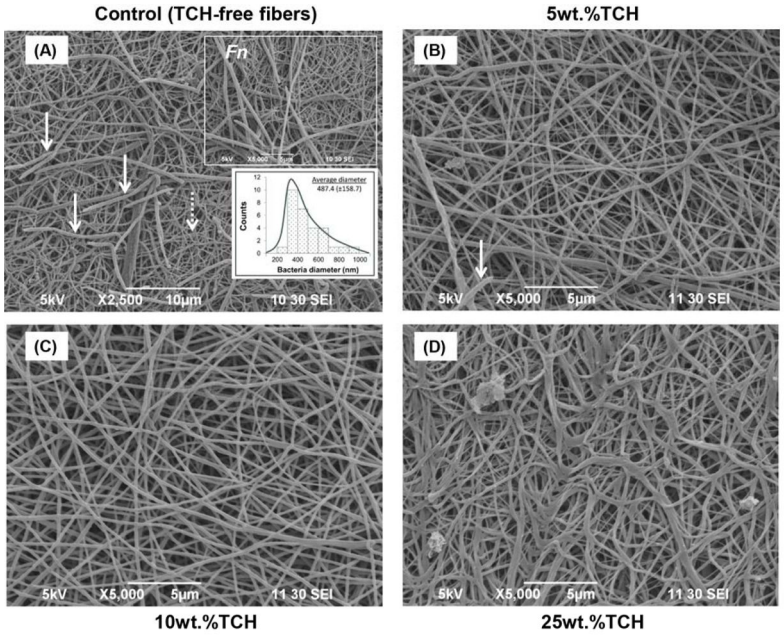

Fig. 4.

Representative SEM images of the electrospun fibers following *Fn* exposure. **(A)** control PLA:PCL/GEL [TCH-free], **(B)** PLA:PCL/GEL+5wt.%TCH, **(C)** PLA:PCL/GEL+10wt.%TCH, and **(D)** PLA:PCL/GEL+25wt.%TCH. **(A)** Note the presence of *Fn* biofilm (solid white arrows) covering most of the nanofibrous (dotted white arrow) surface. Upper inset SEM image (5,000× magnification, scale bar = 5 μm) indicates the morphological aspects of *Fn*. Lower inset graph demonstrates the mean bacterial diameter. **(B)** SEM image demonstrates (white arrow) the presence of *Fn* bacteria only in a few areas on the 5 wt.% of TCH-containing fibers. **(C–D)** SEM images revealing complete absence of *Fn* on the fibers.

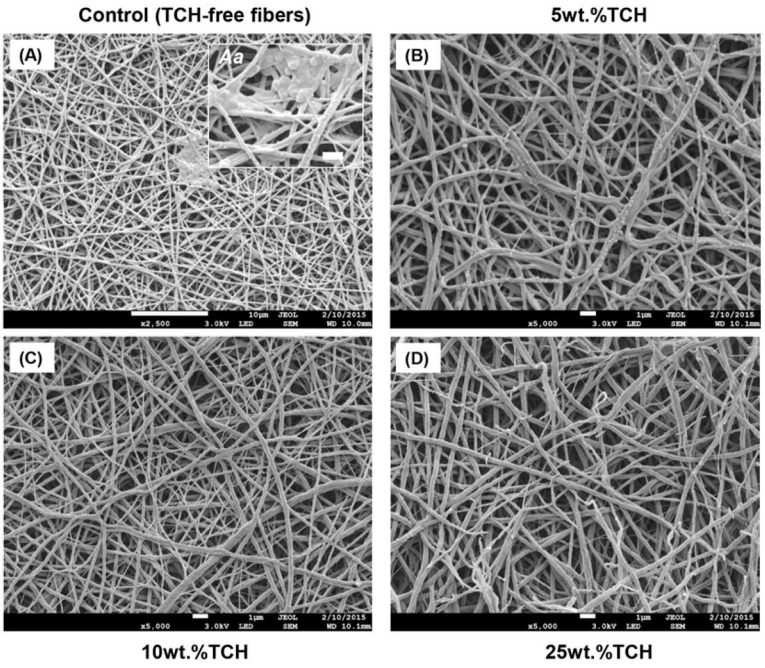

Fig. 5.

Representative SEM images of the electrospun fibers following Aa exposure. **(A)** control PLA:PCL/GEL [TCH-free], **(B)** PLA:PCL/GEL+5wt.%TCH, **(C)** PLA:PCL/GEL+10wt.%TCH, and **(D)** PLA:PCL/GEL+25wt.%TCH. **(A)** Note the presence of *Aa* biofilm covering the nanofibrous surface. Inset SEM image (10,000× magnification, scale bar = 1 μm) demonstrates the morphological aspects of *Aa*. **(B–D)** SEM images revealing complete absence of *Aa* over all TCH-containing fibers.

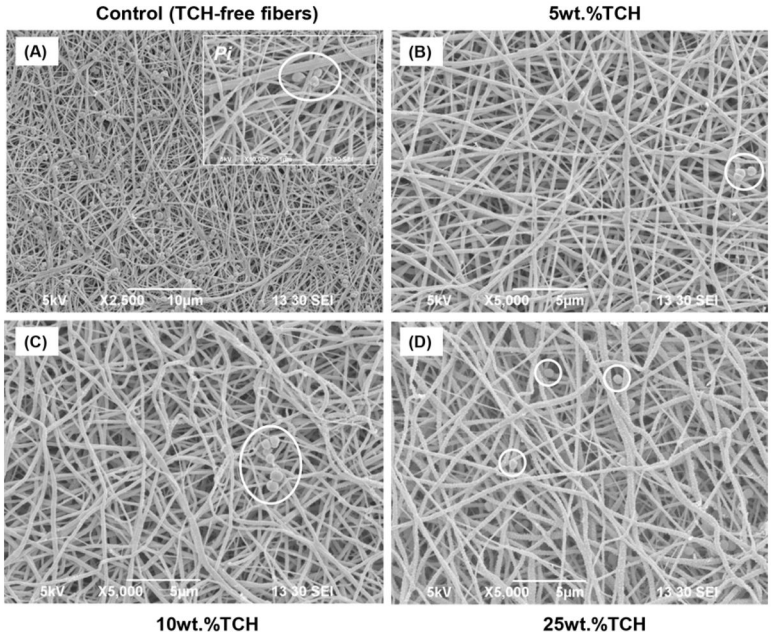

Fig. 6.

Representative SEM images of the electrospun fibers following *Pi* exposure. **(A)** control PLA:PCL/GEL [TCH-free], **(B)** PLA:PCL/GEL+5wt.%TCH, **(C)** PLA:PCL/GEL+10wt.%TCH, and **(D)** PLA:PCL/GEL+25wt.%TCH. **(A)** Note the presence of *Pi* biofilm (white circles) covering most of the nanofibrous surface. Inset SEM image (10,000× magnification, scale bar = 1 μm) demonstrates the morphological aspects of *Pi*. **(B–D)** SEM images revealing a few areas with *Pi* in all TCH-containing fibers.